J Biomol NMR (2015) 62:17–23
DOI 10.1007/s10858-015-9911-1

COMMUNICATION

^{13}C- and ^{1}H-detection under fast MAS for the study of poorly available proteins: application to sub-milligram quantities of a 7 trans-membrane protein

Hugh R. W. Dannatt · Garrick F. Taylor · Krisztina Varga · Victoria A. Higman · Marc-Philipp Pfeil · Lubica Asilmovska · Peter J. Judge · Anthony Watts

Received: 17 December 2014 / Accepted: 14 February 2015 / Published online: 21 February 2015

Abstract We demonstrate that ^{13}C-detected spectra recorded using fast (60 kHz) magic angle spinning on sub-milligram (<10 μmol) quantities of a protonated 7 trans-membrane helix protein (bacteriorhodopsin) in its native lipid environment are comparable in sensitivity and resolution to those recorded using 15-fold larger sample volumes with conventional solid state NMR methodology. We demonstrate the utility of proton-detected measurements which yield narrow ^{1}H linewidths under these conditions, and that no structural alterations are observed. We propose that these methods will prove useful to gain structural information on membrane proteins with poor availability, which can be studied in their native lipid environments.

Keywords 7 trans-membrane proteins · Poorly available proteins · Fast magic angle spinning · Heteronuclear detection · ^{13}C-detection · Low sample volumes

Solid state NMR (ssNMR) is an emerging tool for high-resolution structural studies of proteins. It is particularly attractive for the study of integral membrane proteins (IMPs) (McDermott 2009) which can be probed within a biologically relevant environment, in contrast to solution NMR or X-ray crystallographic studies which require the use of non-native detergents (Warschawski et al. 2011) and are often carried out on highly modified proteins to improve stability or favour crystallisation (Rasmussen et al. 2007; Wernimont and Edwards 2009; Wu et al. 2010). Such modifications may affect the activity and ligand/co-factor binding of membrane proteins (Rosenbaum et al. 2009), and detergents are often destabilising, reducing the physiological relevance of any structures gained for IMPs in non-membrane environments (Cross et al. 2011).

Seven trans-membrane (7TM) proteins are an important class of integral membrane protein that include the pharmacologically important G-protein coupled receptors and the related photoreceptors, archaerhodopsins. Despite the importance of these proteins, either as drug targets (Overington et al. 2006) or in bioengineering (Berthoumieu et al. 2011), few (∼1 % of total) high-resolution structures from unique IMPs are deposited in the protein data bank (www.pdb.org). Indeed, 7TM protein structures are underrepresented in the PDB for several reasons, the major ones being difficulties in availability and purification (Bill et al. 2011).

Despite its utility in membrane protein studies, ssNMR is an inherently insensitive technique and several milligrams of isotopically-labelled proteins are typically required for conventional studies, often rendering low expression levels a significant problem. In addition, the assignment and analysis of signals from ssNMR measurements is often more difficult than for those recorded by solution NMR as a result of low resolution and the difficulties in detecting ^{1}H signals. In recent years, technological advances in concert with smaller sample rotors have enabled magic angle spinning (MAS) frequencies of 60 kHz and above (Agarwal et al. 2013; Ernst et al. 2004),

Hugh R. W. Dannatt and Garrick F. Taylor have contributed equally to this work.

Electronic supplementary material The online version of this article (doi:10.1007/s10858-015-9911-1) contains supplementary material, which is available to authorized users.

H. R. W. Dannatt · G. F. Taylor · K. Varga · V. A. Higman · M.-P. Pfeil · L. Asilmovska · P. J. Judge · A. Watts (✉)
Department of Biochemistry, University of Oxford, South Parks Road, Oxford OX1 3QU, UK
e-mail: anthony.watts@bioch.ox.ac.uk

resulting in much reduced dipolar couplings between nuclei, thereby increasing sensitivity and resolution, and opening up ^{1}H-detection (Marchetti et al. 2012; Zhou et al. 2007a).

The relatively sharp proton linewidths recorded at MAS frequencies of 60 kHz and above give ^{1}H-detected experiments a sensitivity advantage, although spectral resolution in ^{1}H may be insufficient for application to larger systems without the use of perdeuteration of non-exchangeable sites, which may be especially troublesome for IMPs due to inaccessibility of buried amide sites that cannot be readily back-exchanged (Linser et al. 2011b; Ward et al. 2011). In addition, the superior spectral resolution in ^{13}C may be inefficiently sampled as an indirect dimension, while direct detection of ^{13}C spins allows the full resolution to be realised without any cost in experiment time (Guo et al. 2014). Furthermore, by detecting correlations between the side-chain resonances, many more structural restraints are available from ^{13}C-detected studies compared to those detecting ^{1}H signals, which have predominantly been distances between amide protons (Knight et al. 2011; Zhou et al. 2007b). Such distance restraints are limited in their utility for determining the tertiary structures of predominantly α-helical proteins such as the 7TM family, although correlations utilising selectively protonated methyls have also been used more recently (Linser et al. 2011a).

Although principally used for ^{1}H-detection in the solid state, fast MAS rates also provide advantages for ^{13}C-detected experiments, enabling low-power ^{1}H decoupling schemes during frequency-labelling and acquisition periods (Ernst et al. 2001; Vijayan et al. 2009). These low-power schemes reduce or even eliminate radiofrequency (RF) heating of the sample, allowing many more signal acquisitions per unit time without risking sample integrity (Laage et al. 2009). This, along with the inherently more sensitive smaller detection coils employed in fast spinning probes partially compensates the reduced sample volumes used, and as such the application of these techniques allows for high-quality ssNMR spectra to be recorded on very small amounts of protein. This strategy is therefore particularly appealing for the investigation of those membrane proteins that have so far eluded high-resolution structural characterisation due to their low availability.

To date, MAS frequencies of 60 kHz have been successfully applied to perdeuterated (Lewandowski et al. 2011; Zhou et al. 2007b) and protonated (Marchetti et al. 2012) microcrystalline samples, precipitates (Marchetti et al. 2012), and sediments (Bertini et al. 2013). Examples of studies on membrane proteins that either use fast MAS spinning or high levels of perdeuteration to detect ^{1}H signals also exist in the literature (Barbet-Massin et al. 2014; Linser et al. 2011b; Tang et al. 2013; Zhou et al. 2012). Here, we demonstrate that fast MAS can be applied to a fully protonated 7TM protein—bacteriorhodopsin (bR) in its native purple membrane environment—enabling detection on both proton and carbon-13 spins in a sub-milligram sample, comparing favourably with ^{13}C-detected measurements made on larger samples at slower spinning rates, and—crucially—without inducing undesired structural alterations.

1D ^{13}C CP spectra recorded on bR in purple membrane showing the aliphatic resonances at both fast (60 kHz) and slow (10 kHz) sample spinning speeds are shown in Fig. 1. Although the sensitivity of the spectrum recorded at 60 kHz is lower than that of its slow spinning counterpart as a consequence of the much smaller available sample volume, it is seen that the agreement between the peak positions in the spectra is excellent.

NCA and NCO spectra—correlating the backbone amide ^{15}N spin with the adjacent ^{13}C spins—recorded in both spinning regimes are compared in Fig. 2. Both sets of spectra overlay very well, with no significant changes in linewidths or chemical shifts observed between spectra recorded under slow and fast MAS. However, as in the case of the one dimensional ^{13}C spectra, it is seen that the overall sensitivity of the spectra recorded at 60 kHz is lower than that of those recorded at slow spinning.

Homonuclear recoupling methods for recording ^{13}C–^{13}C correlations are a key component of ssNMR analyses of ^{13}C-labelled proteins, but many of the methods that rely on spin diffusion for magnetisation transfer—such as dipolar assisted rotational resonance (DARR) (Takegoshi et al. 2001)—are less effective under fast MAS (Ishii 2001). As such, alternative recoupling schemes were sought. Initially

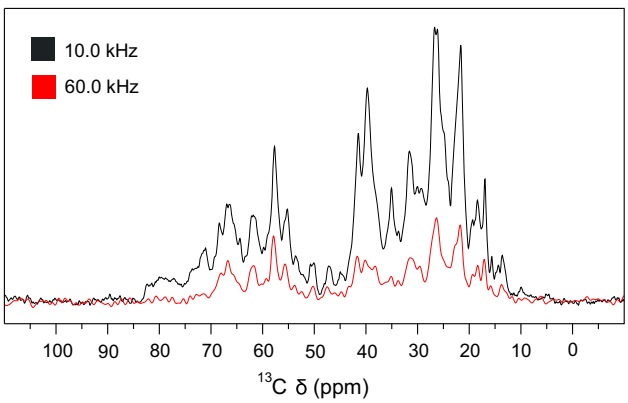

Fig. 1 1D ^{13}C CP spectra recorded at slow (10.0 kHz, *black*) and fast (60 kHz, *red*) magic angle spinning. The total experiment time used for both spectra was approximately 100 s. Although shorter inter-scan delay lengths allow more scans to be recorded per unit time in the fast spinning case, it can be seen that the resulting sensitivity is much lower than that seen from the larger diameter rotors used for slow MAS. All spectra were recorded at 18.8 T with sample temperatures of 0 °C (slow spinning) and 20 °C (fast spinning)

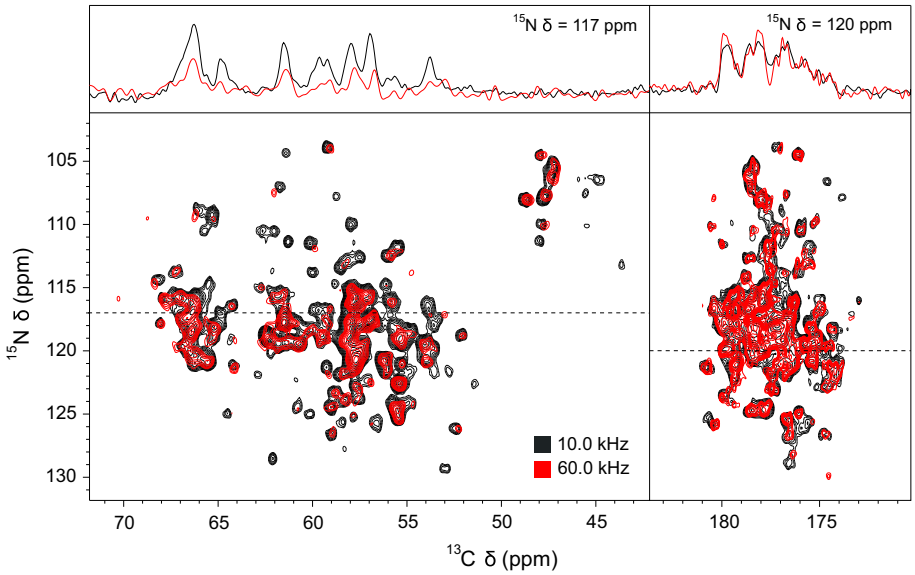

Fig. 2 ^{13}C-detected NCA (*left*) and NCO (*right*) spectra recorded at slow (10.0 kHz, *black*) and fast (60 kHz, *red*) magic angle spinning. Although the NCA recorded at slow spinning is considerably more sensitive than that recorded at 60 kHz MAS, both sets of spectra overlay very well and do not show significant sample changes between spinning regimes. In both cases, the spectra are scaled to adjust for differences in experiment time. Representative 1D slices illustrating relative sensitivity and linewidths are shown above the 2D spectra. All spectra were recorded at 18.8 T with sample temperatures of 0 °C (slow spinning) and 20 °C (fast spinning)

we tried to use the dipolar recoupling enhanced by amplitude modulation (DREAM) scheme (Verel et al. 2001), however this proved difficult to optimise and we instead opted for the more broadband radiofrequency driven recoupling (RFDR) (Bennett et al. 1992) method. RFDR has already been successfully used at fast MAS frequencies to recouple ^{1}H homonuclear dipolar couplings and establish distance constraints for protein structure calculation (Knight et al. 2011; Linser et al. 2011a).

The overlay between the DARR spectrum recorded at slow MAS and the RFDR spectrum recorded at fast MAS is shown in Fig. 3. This comparison is less straightforward than for the NCA/NCO spectra (Fig. 2) given that different recoupling schemes were used, leading to differences in the necessary lengths of the recoupling blocks. Roughly equivalent mixing times were chosen so that the off-diagonal peaks correspond predominantly to one-bond correlations in both cases (15 ms DARR mixing time, vs. 2 ms RFDR mixing time), however it is clear from the spectra that some longer-range correlations are visible in the DARR but not in the RFDR, particularly between the carbonyl and aliphatic side chain resonances. For those peaks that appear in both spectra, the observation is similar to that for the other carbon-detected spectra: the peaks overlay extremely well with no significant changes in signal linewidths or chemical shifts.

Despite the higher sensitivity of the 1.3 mm probe with its smaller sample coil, and the faster repetition rates permitted by the low power ^{1}H decoupling schemes used at fast MAS, it was anticipated that the spectra recorded at fast MAS would be less sensitive than their slow MAS counterparts due to the large reduction in sample volume. The capacity of a Bruker 1.3 mm rotor is 2.5 µl, whereas the Agilent thin-walled 3.2 mm rotor is 15-fold larger, with a volume of 36 µl. The active volumes of the rotors gives an even larger difference between them, with the entire 36 µl detected in the case of the 3.2 mm rotor, but only the central 1.6 µl contributing to the signal in the case of the 1.3 mm Bruker rotor, a factor of 22.5 less. Indeed, the 3.2 mm sample rotor was roughly estimated to contain 3.0–3.4 mg of bacteriorhodopsin, whereas absorbance measurements of the sample used for the fast spinning experiments once removed from the 1.3 mm rotor post-experiment revealed the rotor contained only 250 µg of bacteriorhodopsin, which corresponds to <10 µmol of protein.

Signal:noise measurements show that the NCA spectrum recorded under fast spinning is 2.5-fold less sensitive than that recorded using slow spinning, once the differences in the acquisition times used are taken into account. In the case of the NCO spectra, the spectrum recorded at 60 kHz MAS compares more favourably, since the higher degree of chemical shift anisotropy of the carbonyl resonances leads—at slow spinning—to a significant portion (approx. 40 %) of the signal intensity being contained in the spinning side bands, which are completely collapsed at 60 kHz. The NCO spectrum recorded at 60 kHz MAS is only 1.2-fold less sensitive than that recorded using slow

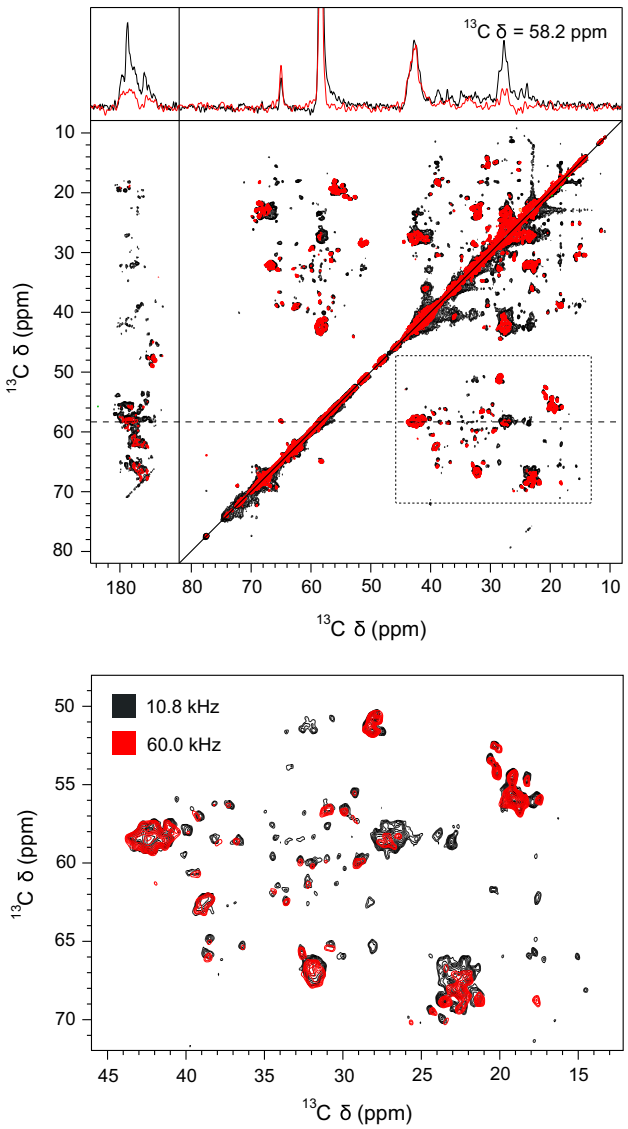

Fig. 3 An overlay of ^{13}C–^{13}C correlation spectra—a DARR spectrum recorded at 10.8 kHz using a 15 ms mixing block (*black*), and an RFDR spectrum recorded at 60 kHz using a 2 ms mixing block (*red*). The entire aliphatic region and the aliphatic-carbonyl cross peak region is shown at the *top*, with the region corresponding predominantly to Cα–Cβ cross peaks shown in detail *below*. A representative 1D slice is shown above the top spectrum to illustrate relative sensitivity and linewidths between spinning regimes. Both spectra were recorded at 18.8 T with sample temperatures of 0 °C (slow spinning) and 20 °C (fast spinning)

spinning frequencies. A meaningful quantitative comparison between the DARR and RFDR spectra is difficult to make, though using the cluster of signals found at approximately 42 × 58 ppm, the RFDR spectrum is 1.2-fold less sensitive than the DARR spectrum. The relative sensitivities of the spectra are remarkable given the large reduction in sample volume in the fast spinning case.

Although not explored here, there has been some recent successes (Ullrich et al. 2014; Ward et al. 2014) in the use of paramagnetic doping of membrane protein samples, which decreases the ^{1}H relaxation time and enables more scans to be acquired per unit time, thereby increasing sensitivity (Wickramasinghe et al. 2007). As the inter-scan delay in the slow MAS case is normally limited by sample and equipment heating, this strategy is best suited to experiments utilising low power pulse schemes at high MAS, and would make experiments carried out under these conditions compare more favourably to those recorded at low MAS rates on larger sample volumes.

Although the overlay between peaks recorded under fast and slow MAS is very good, some small chemical shift changes between the two sets of data can be seen. This is to be expected given that the slow spinning data was recorded at a sample temperature of approx. 0 °C, whilst the sample in the 1.3 mm rotor could only be cooled to approx. 20 °C due to greater frictional heating caused by the faster spinning rate. In addition, there are potential differences in hydration between the two samples, as well as differences in g-forces generated by the spinning sample rotors and the resulting differences in hydrostatic pressure experienced by the sample between the two spinning regimes. In spite of these experimental differences, excellent overlay between spectra recorded in the two spinning regimes is seen (Figs. 1, 2, 3), demonstrating that the sample is not adversely affected by fast spinning. Although bR represents a well-known and resilient example of 7TM proteins, this is an important test for the study of membrane proteins utilising fast MAS speeds, as loss of structure due to the high centripetal forces exerted on the sample has previously been a concern for protein studies (Böckmann 2007), as it has shown to be detrimental in studies of tissue and cell samples by HR-MAS (Wind et al. 2001).

For a more quantitative comparison, we have calculated the centripetal force and pressure experienced by the sample in both spinning regimes, displayed in Table 1. We find that, in terms of the hydrostatic pressure experienced by the sample in both cases, the faster spinning is largely compensated for by the use of smaller rotors. Despite a ten-fold increase in the g-force generated by the faster spinning, only a two-fold increase in the hydrostatic pressure experienced by the sample is expected, from 90 bar at 10 kHz spinning to 210 bar at 60 kHz. Although a pressure two orders of magnitude above atmospheric is not insignificant, it is far below the pressures typically needed for large structural perturbations, such as separation of protein oligomers or complexes into monomeric units (1–2 kbar), and unfolding of monomeric proteins (>5 kbar) (Silva and Weber 1993), with the only effect likely a slight dehydration of the lipid bilayers (Zhou et al. 1999). In addition, although the thin walled 3.2 mm rotor used in this study cannot be spun fast enough to match the pressure generated by the 60 kHz spinning, a thick walled 3.2 mm rotor would

Table 1 Calculated values of centripetal force, and the resulting hydrostatic pressure against the inner wall of the sample rotor, generated by MAS of Bruker 1.3 mm rotors and Agilent 3.2 mm rotors

Rotor type	MAS rate (kHz)	Rotor inner radius (mm)	Acceleration relative to g, a/g	Hydrostatic pressure (bar)
3.2 mm Agilent, thin walled	10.8	1.275	6.0×10^5	90
1.3 mm Bruker, standard	60.0	0.35	5.1×10^6	210
3.2 mm Agilent, thin walled	15.0 (max)	1.275	1.2×10^6	180
3.2 mm Agilent, thick walled	25.0 (max)	1.125	2.8×10^6	380
1.3 mm Bruker, standard	67.0 (max)	0.35	6.3×10^6	260

The two top rows refer to the conditions under which the data contained in this paper was acquired, in both slow and fast spinning regimes used in this study, whereas the bottom three rows refer to the maximum rotation rates of both types of Agilent 3.2 mm rotors and of the Bruker 1.3 mm rotors. Equations used are given in the supporting information

generate nearly twice the pressure experienced by the bR sample in the fast spinning case if the rotor were spun at its experimental limit. Indeed, even a 7 mm rotor exceeds the pressure calculated for the 60 kHz case if it is spun at its maximum frequency. We do not therefore see force and pressure generated by fast MAS as a reason to avoid these experiments in favour of those utilising slower MAS frequencies.

Conversely, high sample temperatures due to frictional heating can represent a problem at high MAS rates. Even with high gas flow rates and the temperature control unit set to 225 K (−48 °C), the bR sample could not be cooled below 20 °C (as determined from the water signal). Although bR in hydrated purple membrane is stable at temperatures up to 80 °C (Hampp 2000), many less stable systems must be cooled below room temperature to prevent degradation over the timescales of these experiments. Sample heating due to friction increases non-linearly with the spinning rate (Dvinskikh et al. 2004; Langer et al. 1999), and as such this limitation could be overcome by reducing the MAS frequency to 55 kHz or even 50 kHz—speeds at which low-power ^{1}H decoupling schemes such as those used here are still effective.

As fast sample spinning frequencies open up ^{1}H-detected experiments, we assessed the proton signal linewidths and the feasibility of ^{1}H-detection for the study of non-deuterated membrane proteins under native conditions by recording ^{1}H-detected HSQC spectra. For the magnetisation transfer steps, we used both dipolar and scalar couplings, which detect ordered and flexible regions of the protein, respectively, as shown in Fig. 4. In the absence of perdeuteration, and in the presence of a fully protonated lipid and solvent background, the resonances detected in the spectrum using dipolar-based transfer steps display remarkably narrow ^{1}H linewidths of <200 Hz. Many more peaks are seen than in the previously published spectrum recorded on highly deuterated bR at 20 kHz spinning, presumably corresponding to membrane-embedded amides that are not accessible to solvent exchange (Linser et al. 2011b). In the spectrum recorded using scalar transfers, very few resonances are detected, showing that only a few isolated regions of the protein are flexible on the chemical

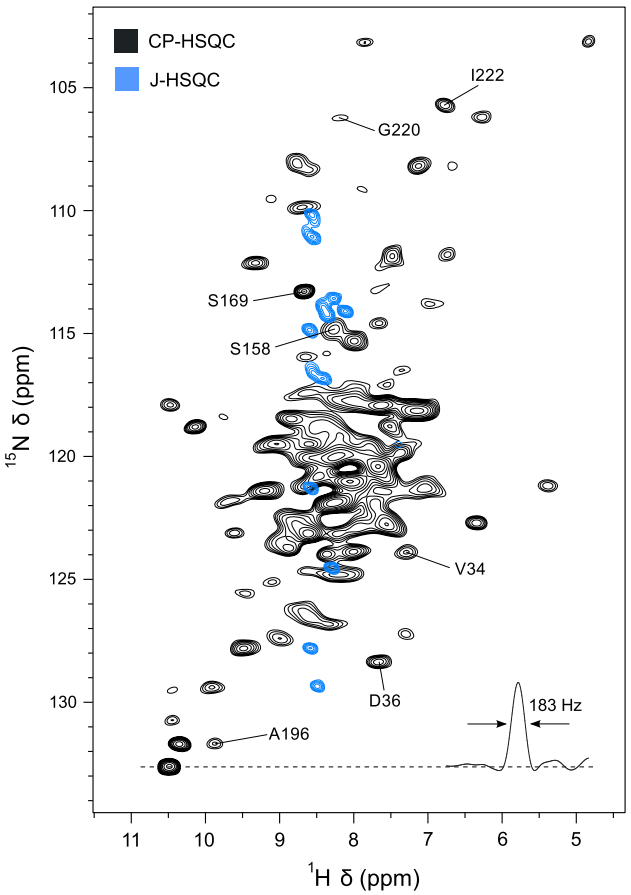

Fig. 4 An overlay of ^{1}H-detected HSQC spectra recorded at 60 kHz, 18.8 T and 20 °C using dipolar-based (CP) magnetisation transfers (*black*), and J-based (INEPT) transfers (*blue*). Few signals are seen in the J-HSQC spectrum, which detects highly mobile regions. Where possible, the resonance assignments have been transferred from the ^{13}C-detected NCA spectrum using the ^{1}H-detected HNCA spectrum as an intermediate. The 1D slice shown is for the most downfield peak in ^{15}N (132.6 ppm)

shift timescale, as has been previously noted by ^{13}C-detected experiments on bR in purple membrane (Higman et al. 2011).

The ^{1}H-detected spectra demonstrate the molecular order which is naturally present in the purple membrane, giving ^{1}H linewidths as narrow as those measured from microcrystalline preparations of protonated soluble proteins (Marchetti et al. 2012). Such narrow ^{1}H linewidths at 60 kHz from a membrane protein in its native environment demonstrate the feasibility of further study using ^{1}H-detected methods to study membrane proteins. We investigated the potential of utilising ^{1}H detection to record 3D spectra in the place of ^{13}C-detected 2D spectra by recording an HNCA spectrum (not shown). Surprisingly, we find that the HNCA spectrum compares poorly to the NCA in terms of sensitivity, with very few additional resonances visible despite a measurement time several times that used for the NCA, and heavily truncated indirect dimensions. The three dimensional spectrum did at least allow the transfer of a handful of resonance assignments, which have previously been assigned by ^{13}C-detected methods (Higman et al. 2011), to the HSQC spectrum, as shown in Fig. 4.

A recent paper by Meier and co-workers has demonstrated that ^{1}H-detected spectra improve significantly in resolution if the MAS rate is increased further to 100 kHz (Agarwal et al. 2014). Due to increased frictional heating, this approach is only likely to be applicable to highly stable proteins unless improved sample cooling systems can be developed. Furthermore, ^{13}C-detected experiments are not expected to improve greatly between 60 and 100 kHz, meaning that overall sensitivity of these measurements will be reduced due to the smaller sample rotor diameter (0.8 mm).

In conclusion, we have demonstrated that high-quality NMR spectra can be recorded on very small (sub-milligram) amounts of bR in its native purple membranes by the use ^{13}C-detected NMR experiments employing low power ^{1}H decoupling at fast MAS frequencies. The excellent overlay of signals between the fast and slow spinning experiments demonstrates that bR retains its structure in the fast-spinning case, providing an important proof of principle for membrane protein studies using ssNMR with fast MAS. Although the spectra recorded at 60 kHz MAS are less sensitive than their counterparts recorded at slower spinning frequencies, the reduction in signal:noise is small compared to the large difference in sample requirements (approx. 15-fold less material), demonstrating that this is a viable method to study membrane proteins of low availability. Furthermore, we have shown that fully protonated bR in purple membranes gives relatively narrow (<200 Hz) ^{1}H linewidths at 60 kHz MAS, demonstrating the potential for ^{1}H-detected studies on fully protonated 7-helix transmembrane proteins in a native environment.

Acknowledgments We gratefully acknowledge funding from the Medical Research Council (MRC), the Biotechnology and Biological Sciences Research Council (BBSRC), and the Engineering and Physical Sciences Research Council (EPSRC). We acknowledge the BioNMR initiative (EC-FP7 Project Number: 261863) for funding access to the CRMN facility in Lyon where all 60 kHz MAS data was recorded, and we thank Moreno Lelli for his assistance during these visits. We acknowledge the use of the solid state NMR facility at the University of Warwick where preliminary fast spinning NMR data was recorded.

Conflict of interest The authors declare no conflict of interest.

References

Agarwal V, Tuherm T, Reinhold A, Past J, Samoson A, Ernst M, Meier BH (2013) Amplitude-modulated low-power decoupling sequences for fast magic-angle spinning NMR. Chem Phys Lett 583:1–7

Agarwal V et al (2014) De Novo 3D structure determination from sub-milligram protein samples by solid-state 100 kHz MAS NMR spectroscopy. Angew Chem Int Ed 53:12253–12256

Barbet-Massin E et al (2014) Rapid proton-detected NMR assignment for proteins with fast magic angle spinning. J Am Chem Soc 136:12489–12497

Bennett AE, Griffin RG, Ok JH, Vega S (1992) Chemical shift correlation spectroscopy in rotating solids: radio frequency-driven dipolar recoupling and longitudinal exchange. J Chem Phys 96:8624

Berthoumieu O, Patil AV, Xi W, Aslimovska L, Davis JJ, Watts A (2011) Molecular scale conductance photoswitching in engineered bacteriorhodopsin. Nano Lett 12:899–903

Bertini I, Luchinat C, Parigi G, Ravera E (2013) SedNMR: on the edge between solution and solid-state NMR. Acc Chem Res 46:2059–2069

Bill RM et al (2011) Overcoming barriers to membrane protein structure determination. Nat Biotech 29:335–340

Böckmann A (2007) High-resolution solid-state MAS NMR of proteins—Crh as an example. Magn Reson Chem 45:S24–S31

Cross TA, Sharma M, Yi M, Zhou H-X (2011) Influence of solubilizing environments on membrane protein structures. Trends Biochem Sci 36:117–125

Dvinskikh SV, Castro V, Sandström D (2004) Heating caused by radiofrequency irradiation and sample rotation in ^{13}C magic angle spinning NMR studies of lipid membranes. Magn Reson Chem 42:875–881

Ernst M, Samoson A, Meier BH (2001) Low-power decoupling in fast magic-angle spinning NMR. Chem Phys Lett 348:293–302

Ernst M, Meier MA, Tuherm T, Samoson A, Meier BH (2004) Low-power high-resolution solid-state NMR of peptides and proteins. J Am Chem Soc 126:4764–4765

Guo C, Hou G, Lu X, O'Hare B, Struppe J, Polenova T (2014) Fast magic angle spinning NMR with heteronucleus detection for resonance assignments and structural characterization of fully protonated proteins. J Biomol NMR 60:219–229

Hampp N (2000) Bacteriorhodopsin as a photochromic retinal protein for optical memories. Chem Rev 100:1755–1776

Higman VA, Varga K, Aslimovska L, Judge PJ, Sperling LJ, Rienstra CM, Watts A (2011) The conformation of bacteriorhodopsin loops in purple membranes resolved by solid-state MAS NMR spectroscopy. Angew Chem Int Ed 50:8432–8435

Ishii Y (2001) ^{13}C–^{13}C dipolar recoupling under very fast magic angle spinning in solid-state nuclear magnetic resonance:

applications to distance measurements, spectral assignments, and high-throughput secondary-structure determination. J Chem Phys 114:8473–8483

Knight MJ et al (2011) Fast resonance assignment and fold determination of human superoxide dismutase by high-resolution proton-detected solid-state MAS NMR spectroscopy. Angew Chem Int Ed 123:11901–11905

Laage S, Sachleben JR, Steuernagel S, Pierattelli R, Pintacuda G, Emsley L (2009) Fast acquisition of multi-dimensional spectra in solid-state NMR enabled by ultra-fast MAS. J Magn Reson 196:133–141

Langer B, Schnell I, Spiess HW, Grimmer A-R (1999) Temperature calibration under ultrafast MAS conditions. J Magn Reson 138:182–186

Lewandowski JR, Dumez J-N, Akbey Ü, Lange S, Emsley L, Oschkinat H (2011) Enhanced resolution and coherence lifetimes in the solid-state NMR spectroscopy of perdeuterated proteins under ultrafast magic-angle spinning. J Phys Chem Lett 2:2205–2211

Linser R, Bardiaux B, Higman V, Fink U, Reif B (2011a) Structure calculation from unambiguous long-range amide and methyl ^{1}H–^{1}H distance restraints for a microcrystalline protein with MAS solid-state NMR spectroscopy. J Am Chem Soc 133:5905–5912

Linser R et al (2011b) Proton-detected solid-state NMR spectroscopy of fibrillar and membrane proteins. Angew Chem Int Ed 50:4508–4512

Marchetti A et al (2012) Backbone assignment of fully protonated solid proteins by ^{1}H detection and ultrafast magic-angle-spinning NMR spectroscopy. Angew Chem Int Ed 124:10914–10917

McDermott A (2009) Structure and dynamics of membrane proteins by magic angle spinning solid-state NMR. Annu Rev Biophys 38:385–403

Overington JP, Al-Lazikani B, Hopkins AL (2006) How many drug targets are there? Nat Rev Drug Discov 5:993–996

Rasmussen SGF et al (2007) Crystal structure of the human [bgr]2 adrenergic g-protein-coupled receptor. Nature 450:383–387

Rosenbaum DM, Rasmussen SGF, Kobilka BK (2009) The structure and function of G-protein-coupled receptors. Nature 459:356–363

Silva J, Weber G (1993) Pressure stability of proteins. Annu Rev Phys Chem 44:89–113

Takegoshi K, Nakamura S, Terao T (2001) ^{13}C–^{1}H dipolar-assisted rotational resonance in magic-angle spinning NMR. Chem Phys Lett 344:631–637

Tang M, Comellas G, Rienstra CM (2013) Advanced solid-state NMR approaches for structure determination of membrane proteins and amyloid fibrils. Acc Chem Res 46:2080–2088

Ullrich SJ, Hölper S, Glaubitz C (2014) Paramagnetic doping of a 7TM membrane protein in lipid bilayers by Gd^{3+}-complexes for solid-state NMR spectroscopy. J Biomol NMR 58:27–35

Verel R, Ernst M, Meier BH (2001) Adiabatic dipolar recoupling in solid-state NMR: the DREAM scheme. J Magn Reson 150:81–99

Vijayan V, Demers J-P, Biernat J, Mandelkow E, Becker S, Lange A (2009) Low-power solid-state NMR experiments for resonance assignment under fast magic-angle spinning. Chem Phys Chem 10:2205–2208

Ward ME, Shi L, Lake E, Krishnamurthy S, Hutchins H, Brown LS, Ladizhansky V (2011) Proton-detected solid-state NMR reveals intramembrane polar networks in a seven-helical transmembrane protein proteorhodopsin. J Am Chem Soc 133:17434–17443

Ward ME, Wang S, Krishnamurthy S, Hutchins H, Fey M, Brown LS, Ladizhansky V (2014) High-resolution paramagnetically enhanced solid-state NMR spectroscopy of membrane proteins at fast magic angle spinning. J Biomol NMR 58:37–47

Warschawski DE, Arnold AA, Beaugrand M, Gravel A, Chartrand É, Marcotte I (2011) Choosing membrane mimetics for NMR structural studies of transmembrane proteins. BBA-Biomembranes 1808:1957–1974

Wernimont A, Edwards A (2009) In situ proteolysis to generate crystals for structure determination: an update. PLoS One 4:e5094

Wickramasinghe NP, Kotecha M, Samoson A, Past J, Ishii Y (2007) Sensitivity enhancement in ^{13}C solid-state NMR of protein microcrystals by use of paramagnetic metal ions for optimizing ^{1}H T_1 relaxation. J Magn Reson 184:350–356

Wind RA, Hu JZ, Rommereim DN (2001) High-resolution ^{1}H NMR spectroscopy in organs and tissues using slow magic angle spinning. Magnet Reson Med 46:213–218

Wu B et al (2010) Structures of the CXCR4 chemokine GPCR with small-molecule and cyclic peptide antagonists. Science 330:1066–1071

Zhou Z, Sayer BG, Hughes DW, Stark RE, Epand RM (1999) Studies of phospholipid hydration by high-resolution magic-angle spinning nuclear magnetic resonance. Biophys J 76:387–399

Zhou DH, Shah G, Cormos M, Mullen C, Sandoz D, Rienstra CM (2007a) Proton-detected solid-state NMR spectroscopy of fully protonated proteins at 40 kHz magic-angle spinning. J Am Chem Soc 129:11791–11801

Zhou DH et al (2007b) Solid-state protein-structure determination with proton-detected triple-resonance 3D magic-angle-spinning NMR spectroscopy. Angew Chem Int Ed 46:8380–8383

Zhou D et al (2012) Solid-state NMR analysis of membrane proteins and protein aggregates by proton detected spectroscopy. J Biomol NMR 54:291–305